Article ID: 1003－6326(2005)03－0653－08

Effect of preparation conditions on properties of Al-substituted α-Ni(OH)$_2$ prepared by homogeneous precipitation①

ZHANG Qian(张 倩)[1], XU Yan-hui(徐艳辉)[1, 2],
WANG Xiao-lin(王晓琳)[1], HE Guo-rong(何国荣)[1]
(1. Department of Chemical Engineering, Tsinghua University, Beijing 100084, China;
2. Fuel Science Laboratory Faculty of Mechanic Engineering and Production,
Hamburg University of Applied Sciences, 20099, Hamburg, Germany)

Abstract: Al-substituted α-Ni(OH)$_2$ was synthesized under different reaction conditions by a homogeneous precipitation method. The effect of reaction temperature, reaction time, Ni and Al ions concentration and reagent ratio on the physico-chemical properties and electrochemical performance of Al-substituted α-Ni(OH)$_2$ was studied. The Al-substituted α-Ni(OH)$_2$ samples were characterized by X-ray diffractometry(XRD), infrared spectrometry(FT-IR), inductively coupled plasma(ICP), thermogravimetry(TG) and electrochemical test. The results reveal that the physico-chemical properties and electrochemical performance of the sample are influenced strongly by the preparation conditions. Keeping reaction temperature at 100 or 104 ℃ is appropriate and the largest specific discharge capacity of the sample is 320 mA·h/g. With the reaction time increasing, the discharge capacity increases first and then decreases slightly. It is appropriate that the Ni and Al ions concentration and the ratio of urea to Ni and Al ions are 0.42 mol/L and 0.75∶1, respectively.

Key words: homogeneous precipitation method; α-Ni(OH)$_2$; Ni/MH batteries; electrochemical performance
CLC number: O 646.54 **Document code:** A

1 INTRODUCTION

Nickel hydroxide is widely used as the positive electrode material of Ni-MH, Ni-Cd and Ni-Zn batteries. It crystallizes in two polymorphic forms known as α-Ni(OH)$_2$ and β-Ni(OH)$_2$. During electrochemical cycles, there are two reversible reactions of nickel hydroxide, namely, α(Ⅱ) ⇌ γ(Ⅲ) and β(Ⅱ) ⇌ β(Ⅲ), respectively[1]. However, γ-NiOOH forms in the long cycling process of β(Ⅱ) ⇌ β(Ⅲ), which results in the mechanical expansion and poor electrode properties due to different interlaminar distances between γ-NiOOH and β-NiOOH[2]. The mechanical expansion can be avoided if α-Ni(OH)$_2$ is used as the electrode material. It is not stable, however, in alkaline solution and can transfer to β-Ni(OH)$_2$. Recently, it has been found that substituting some Ni atoms with Co, Al, Mn can stabilize α-Ni(OH)$_2$[3-7]. In addition, with the rapid development of hydrogen storage alloys[8-11], the positive electrode becomes the main limiting factor to increase the capacity of Ni-MH battery. So much attention has been paid to improving the properties of the positive electrode. Moreover, compared with β-Ni(OH)$_2$, α-Ni(OH)$_2$ has larger specific capacity.

The main preparation methods of α-Ni(OH)$_2$ include direct precipitation[5-7], electrochemical deposition[3] and 'Chimie douce' method[4]. For direct precipitation method, the supersaturation of solution is difficult to control and consequently fine colloid particles prefer to emerge, which results in difficult filtration. Electrochemical deposition method is mainly used in laboratory. 'Chimie douce' method involves a high-temperature step and the sample particle prepared by this method is large and its electrochemical performance is poor. For homogeneous precipitation, by controlling the concentration of reagents, the precipitation reaction proceeds almost in equilibrium state. This method is extensively used in preparing metal oxides[12, 13]. Akinc et al[14] prepared α-Ni(OH)$_2$ material using this method but did not report its electrochemical performance. Xia and Wei[15] used this method to prepare β-Ni(OH)$_2$, but the mixture of α-Ni(OH)$_2$ and β-Ni(OH)$_2$ material was obtained. In previous paper[16] we prepared single α-Ni(OH)$_2$ phase by homogeneous precipitation method. In this paper, the effect of preparation conditions on the physico-chemical properties and electrochemical performance of Al-substituted α-Ni(OH)$_2$ prepared by the homogeneous precipitation method was investigated.

① **Foundation item:** Project(2003CB615701) supported by the National Basic Research Program of China
Received date: 2004－06－01; **Accepted date:** 2004－12－22
Correspondence: WANG Xiao-lin, Professor; Tel: +86-10-62794741; E-mail: xlwang@tsinghua.edu.cn

2 EXPERIMENTAL

2.1 Synthesis of Al-substituted α-Ni(OH)$_2$

The Al-substituted α-Ni(OH)$_2$ was prepared by homogeneous precipitation method which was described in our previous paper[16]. In brief, $Ni(NO_3)_2$ solution, $Al(NO_3)_3$ solution and urea solution were mixed in reaction container and Ni/Al molar ratio was 4∶1. Under the controlled reaction temperature, the mixed solution was stirred continually. Obtained precipitate was washed several times with deionized water to neutralization and filtered. Then the cake was dried in air.

2.2 Physical characterization of samples

The crystal structure of the samples was determined by X-ray diffraction(XRD) analysis using a BRUKER D8 advanced X-ray diffractometer with Cu K_α radiation, at a scanning rate of 3(°)/min and a scanning range of 5°-80°(2θ). The infrared spectroscopy of the samples was studied using a Perkin-Elmer Spectrum GX infrared Spectrophotometer. Thermogravimetric analyses were performed using a WCT-2A thermal analyzer and heating from 30 to 600 ℃ at a rate of 5 ℃/min in the N_2. A Prodigy Leeman ICP-OES was used for the inductively coupled plasma analyses to determine Al-contents.

2.3 Preparation of nickel electrodes and their electrochemical test

The pasted nickel electrodes were prepared as follows: 70% nickel hydroxide and 15% acetylene black powder or carbon powder were mixed thoroughly with 15% ploy(tetrafluoroethylene) emulsion(mass fraction). The paste obtained was incorporated into nickel foam with a spatula. The pasted nickel electrodes were dried and then pressed under a pressure of 20 MPa for 2 min. Thereafter, the electrodes were soaked in 7 mol/L KOH for 24 h before being coupled with foam nickel electrodes on either side as counter electrodes and Hg/HgO electrodes as reference electrodes. Galvanostatic charge-discharge studies were conducted on LAND series battery system instrument (made in China). The working electrode was galvanostatically charged to 1.2C (C is the discharge capacity) at rate of 120 mA/g, set for 5 min, and then discharged at rate of 60 mA/g to 0.2 V vs Hg/HgO/7 mol/L KOH electrode. It is charged with the current density of 120 mA/g. Electrochemical impedance spectroscopy (EIS) was performed using EG&G PARC Model 283 Potentioatat/Galvanostat and Model 1025 Frequency Analyzer. The measurements were made at open circuit potential with a superimposed 5 mV sinusoidal voltage in the frequency range of 100 kHz-5 mHz. Electrochemical impedance system software (Model 398) was used to collect data. The data for the real and imaginary components were analyzed using Equivcrt Software.

3 RESULTS AND DISCUSSION

In homogeneous precipitation reaction, urea is used as the precipitator. It decomposes at high temperature according to following well established reaction[17]:

$$(NH_2)_2CO + 2H_2O \rightarrow 2NH_4OH + CO_2 \quad (1)$$

The decomposition of urea is influenced by reaction temperature, reaction time and the ratio of reagents, so the concentration of OH^-, i.e. the supersaturation of the solution, is influenced by the reaction conditions. Consequently, the reaction conditions strongly influence the physico-chemical properties and electrochemical performance of Al-substituted α-Ni(OH)$_2$. In this paper, the influence of reaction time, reaction temperature and reagent ratios on the physicochemical properties and electrochemical performance of Al-substituted α-Ni(OH)$_2$ was investigated.

3.1 Effect of reaction temperature

The reaction temperature was set as 90, 95, 100 and 104 ℃ (the solution boils at 104 ℃), respectively. At the same time the ratio of urea to nickel and aluminum ions is kept at 1∶1 and the reaction time is 16 h.

The XRD patterns of samples prepared at different reaction temperatures are shown in Fig. 1. The peaks at 2θ= 11.12° and 22.36° are the characteristic peaks of α-Ni(OH)$_2$ material and the three peaks at 35°-47° correspond to the turbostratic structure of α-Ni(OH)$_2$. The diffraction peaks are narrow and sharp which are almost the same as those of samples prepared by 'Chimie douce' method[4]. The XRD data calculated from the XRD patterns are listed in Table 1. With the increase of reaction temperature the interlaminar distance and the distance of c-axis increase and the full width at half maximum (FWHM) of peak (003) decreases. The increase of the interlaminar distance is attribu-

Table 1 XRD data of Al-substituted α-Ni(OH)$_2$

Reaction temperature/ ℃	d_{003}/ Å	$d_{c\,\mathrm{axis}}$/ Å	FWHM of peak(003)/(°)
90	7.823	23.471	1.10
95	7.879	23.638	0.67
100	7.907	23.722	0.57
104	7.950	23.850	0.50

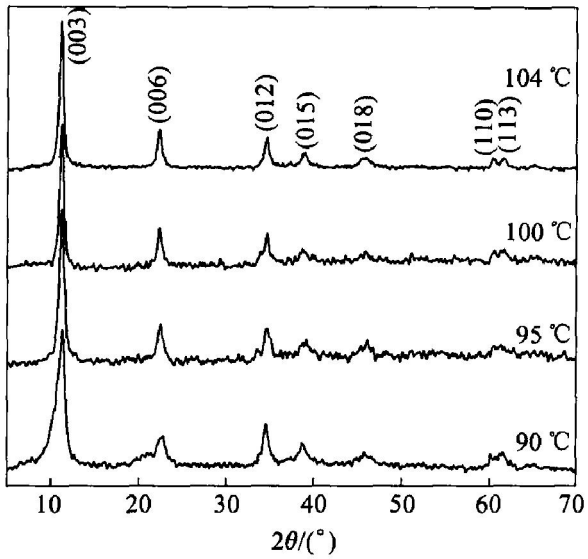

Fig. 1 XRD patterns of Al-substituted α-Ni(OH)$_2$ prepared at different reaction temperatures

ted to weaker electrostatic interaction between the sheets. And the decrease of the FWHM of peak (003) suggests that crystallite grows larger. At higher reaction temperature reagents molecules react and microcrystal congregates easier. Therefore, higher reaction temperature is in favor of crystallite growth.

Fig. 2 shows the FT-IR pattern of sample prepared at 377 K. The broad peak at 3 500 cm^{-1} and weak peak at 1 650 cm^{-1} represent the stretching vibration and bending vibration of water molecular adsorbed or intercalated. The broad peaks at 1 300 - 1 600 cm^{-1} correspond to vibration of CO_3^{2-} and NO_3^- ions. The peaks appearing at 2 230 cm^{-1} and 640 cm^{-1} correspond to the vibration of NCO^- functional group connected with Ni atoms which origins from urea hydrolysis. The peak at 570 cm^{-1} is due to the stretching vibration of M—O band, including Al—O and Ni—O.

Thermogravimetric analysis results of Al-substituted α-Ni(OH)$_2$ prepared at 104 and 90 ℃ are shown in Fig. 3. There are two steps of mass loss for both samples. The first thermogravimetric step represents the loss of adsorbed water or intercalated water. The mass loss at first step is 10.5% and 23.4% (mass fraction) for samples prepared at 104 ℃ and 90 ℃, respectively. The second step corresponding to the decomposition of Ni(OH)$_2$ to NiO emerged at about 250 and 300 ℃ and the mass loss is 21.1% and 25.4% (mass fraction) for samples prepared at 104 ℃ and 90 ℃, respectively. It can be seen that there is more absorbed and intercalated water in the sample prepared at 90 ℃. And the reason for that the sample prepared at 90 ℃ is more stable may be stronger electrostatic action between laminar caused by higher Al/Ni ratio(Table 2) leading to more excessive positive

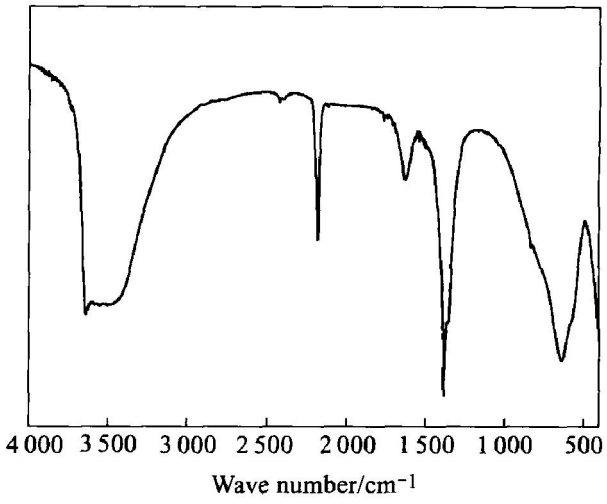

Fig. 2 FT-IR spectrum of Al-substituted α-Ni(OH)$_2$ prepared at 104 ℃

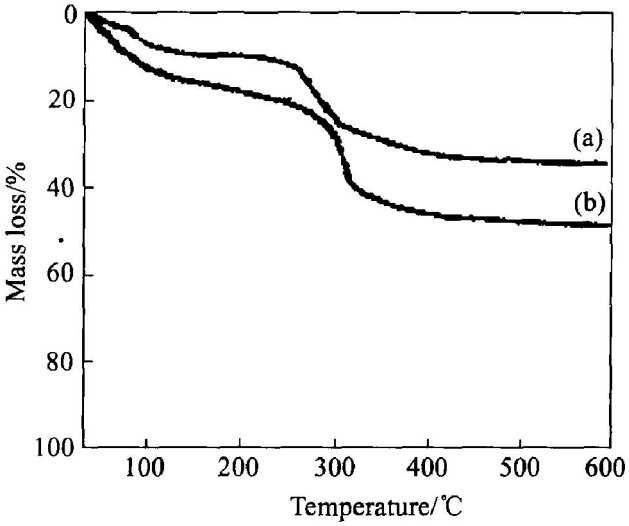

Fig. 3 Thermogravimetric analysis of Al-substituted α-Ni(OH)$_2$ prepared at different temperatures
(a) —104 ℃; (b) —90 ℃

Table 2 ICP and NEE data of Al-substituted α-Ni(OH)$_2$

Reaction temperature/ ℃	Ni/Al ratio	w(Ni)/ %	w(Al)/ %	$N_{EE,\ max}$	$N_{EE,\ av}$
90	1.721∶1	34.87	9.31	1.495	1.453
104	3.684∶1	46.95	5.86	1.474	1.417

charge.

The charge-discharge curves of samples prepared at different temperatures are shown in Fig. 4. With the reaction temperature increasing from 90 ℃ to 100 ℃, the discharge capacity increases, and further increasing the temperature to 104 ℃, the capacity changes slightly. The charging-potential plateau becomes lower and flatter with the reaction temperature increasing. For material prepared at 90 ℃, after 150 mA · h/g, the

charging potential increases slightly. This phenomenon implies that increasing reaction temperature is in favor of increasing the diffusion rate of the proton.

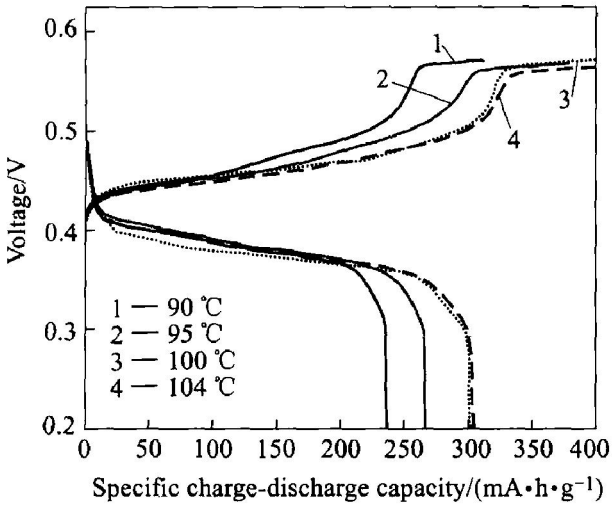

Fig. 4 Charge-discharge curves of Al-substituted α-Ni(OH)$_2$ prepared at different reaction temperatures

The Ni and Al contents of Al-substituted α-Ni(OH)$_2$ prepared at 90 and 104 ℃ are determined by ICP analyses and the number of exchange electron (N_{EE}) per nickel atom is calculated(Table 2). The N_{EE} for each sample was calculated using the formula:

$$N_{EE} = 3\,600C_{exp}/nF \quad (2)$$

where C_{exp} is the experimental discharge capacity in A · h · g^{-1} of sample in the electrode, n is the amount of substance of nickel per gram of sample, and F is Faraday's constant (9 6485 C · mol^{-1}).

It can be seen that the reaction temperature strongly influences the physiochemical properties and electrochemical performance of Al-substituted α-Ni(OH)$_2$. The Ni content of sample prepared at 90 ℃ is 34. 87% (mass fraction) and the Ni/Al molar ratio is 1. 721∶ 1, which is far lower than the ratio 4∶ 1 in reaction solution. In the sample prepared at 104 ℃, Ni content increases to 46. 95% (mass fraction) and the Ni/Al molar ratio is 3. 684∶ 1, which is close to that in reaction solution. Both N_{EE} of samples prepared at 90 and 104 ℃ are about 1. 4. This implies that the influence of reaction temperature on specific discharge capacity is mainly assigned to its influence on the Ni contents in samples. On one hand, Ni content influences virtual active substance content in the sample because Al^{3+} does not take part in oxidation-reduction reaction and does not contribute to capacity. Therefore high Ni content is in favor of large capacity. On the other hand, Ni content influences the distortion of lattice. And because Al(OH)$_3$ solubility is higher than Ni(OH)$_2$, more Al^{3+} ions precipitate at lower pH value. At lower temperature, less urea decomposes and pH value is lower leading to higher Al/Ni ratio in the sample. When the Al/Ni ratio is too high the crystal lattice distorts, the motion of protons are baffled and consequently discharge capacity decreases. On the contrary, more urea decomposes at higher temperature leading to more OH^- ions, so more Ni^{2+} ions can precipitate, Ni content in the sample increases, the crystal lattice is regular and the discharge capacity of sample increases.

3. 2 Effect of reaction time

The charge-discharge curves of Al-substituted α-Ni(OH)$_2$ prepared at 104 ℃ for 4 h, 8 h, 12 h and 16 h are shown in Fig. 5. The ratio of (Ni+Al) ions to urea is 1∶ 1. As the reaction time increases, the discharge capacity increases first and then decreases slightly. The largest discharge capacity 320 mA · h/g is obtained when the reaction time increases to 12 h. It can be seen that with the reaction time increasing from 4 h to 8 h, the charge plateaus become flatter and the discharge potential increases slightly. When the reaction time increases to 12 h, the charge potential changes scarcely and the discharge potential increases continually. But reaction for 16 h, discharge potential decreases slightly and charge potential is invariable.

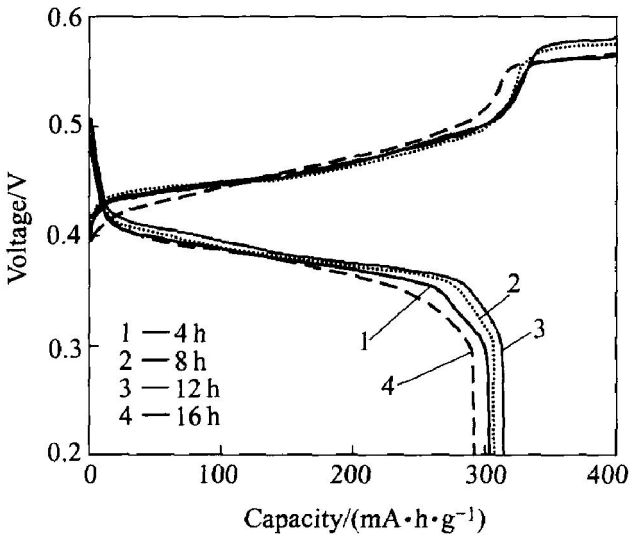

Fig. 5 Charge-discharge curves of Al-substituted α-Ni(OH)$_2$ prepared for different reaction times

The XRD patterns (Fig. 6) show that for longer reaction time, the (110) and (113) diffraction peaks are more clear and distinct, which suggests that the crystallinity of sample becomes higher.

3. 3 Effect of reagent concentration

The charge-discharge curves of Al-substituted α-Ni(OH)$_2$ prepared at 0. 21 mol/L, 0. 42 mol/L,

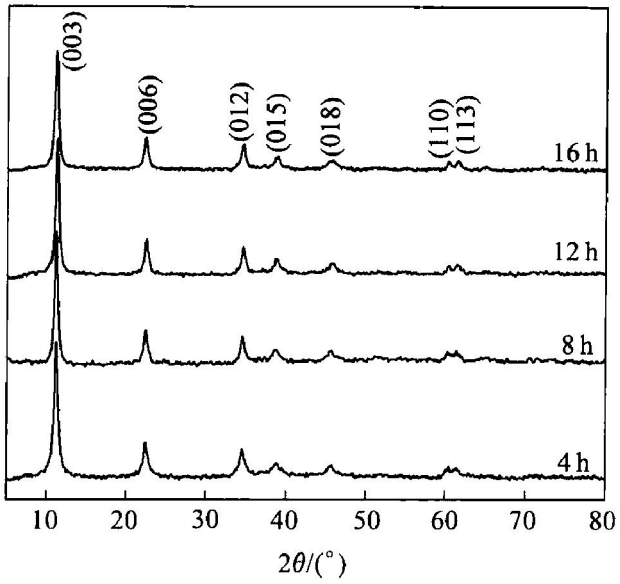

Fig. 6 XRD patterns of Al-substituted α-Ni(OH)$_2$ prepared for different reaction times

0.63 mol/L and 0.84 mol/L (Ni+ Al) ions concentration are shown in Fig. 7. Other preparation conditions, the reaction temperature 104 ℃, the ratio of urea to (Ni+ Al) ions 1∶1 and the reaction time 4 h, are used. It is shown that the concentration of (Ni+ Al) ions has strong influence on the discharge capacity of Al-substituted α-Ni(OH)$_2$. At lower (Ni+ Al) ions concentration, the discharge capacities of samples are larger. As the (Ni+ Al) ions concentration decreases from 0.84 mol/L to 0.63 mol/L, the discharge capacity increases to more than 20 mA · h/g. And with decreasing the (Ni+ Al) ions concentration to 0.42 mol/L, the discharge capacity increases further but the increasing amplitude becomes low. The discharge capacity, however, decreases slightly with the (Ni+ Al) ions concentration decreasing to 0.21 mol/L.

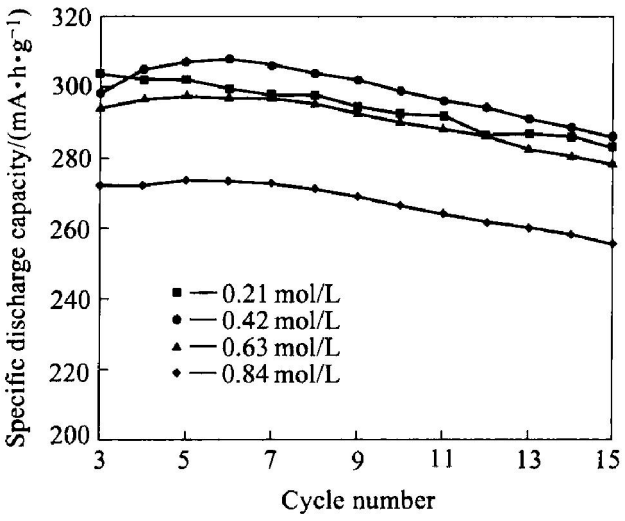

Fig. 7 Specific discharge capacity of Al-substituted α-Ni(OH)$_2$ prepared at different Ni and Al ion concentrations

The (Ni+ Al) ions concentration influence on discharge capacity is mainly assigned to its influence on the Ni content. Table 3 lists the ICP results and the number of exchange electron(N_{EE}) per nickel atom. It can be seen that the Ni/Al molar ratio in Al-substituted α-Ni(OH)$_2$ is near 4∶1 in reaction solution when the (Ni+ Al) ions concentration is in the range of 0.21 – 0.63 mol/L. But when the (Ni+ Al) ions concentration is 0.84 mol/L, the Ni/Al molar ratio deviates far from 4∶1. The number of exchange electron(N_{EE}) per nickel atom is more than 1.3. However, the Ni content is lower leading to lower discharge capacity and the reason is the same as above stated.

Table 3 ICP and NEE data of Al-substituted α-Ni(OH)$_2$

(Ni+ Al) ions concentration/ (mol · L^{-1})	Ni/Al ratio	w(Ni)/ %	w(Al)/ %	$N_{EE,\ max}$	$N_{EE,\ av}$
0.21	4.842∶1	41.69	3.96	1.601	1.560
0.42	3.817∶1	46.46	5.59	1.442	1.409
0.63	4.435∶1	46.76	4.84	1.391	1.358
0.84	2.664∶1	38.61	6.66	1.553	1.529

The charge-discharge curves of Al-substituted α-Ni(OH)$_2$ prepared at different (Ni+ Al) ion concentrations are shown in Fig. 8. With the decrease of (Ni+ Al) ions concentration, the discharge potential increases slightly at the medium and end of discharging and the charge potential decreases slightly. Generally, reagent concentration has a little effect on the charge-discharge curves of the samples.

The XRD patterns of Al-substituted α-Ni(OH)$_2$ original sample and after charge-discharge cycling are recorded (Fig. 9) to test the

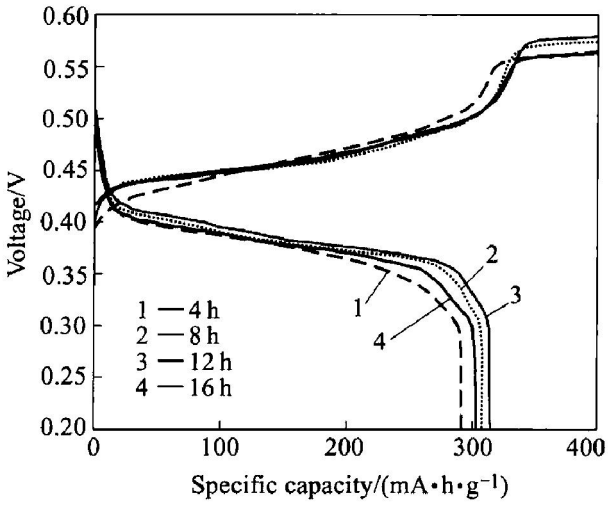

Fig. 8 Charge-discharge curves of Al-substituted α-Ni(OH)$_2$ prepared at different (Ni+ Al) ions concentrations

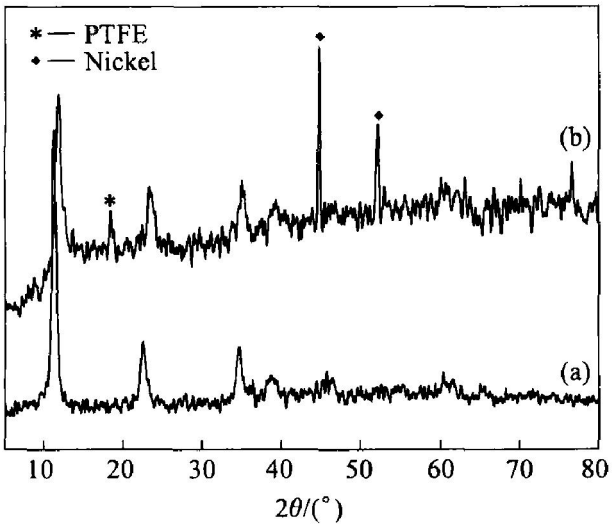

Fig. 9 XRD patterns of Al-substituted α-Ni(OH)$_2$ prepared at 0.42 mol/L (Ni+ Al) ions concentration
(a) —Original sample; (b) —After cycling

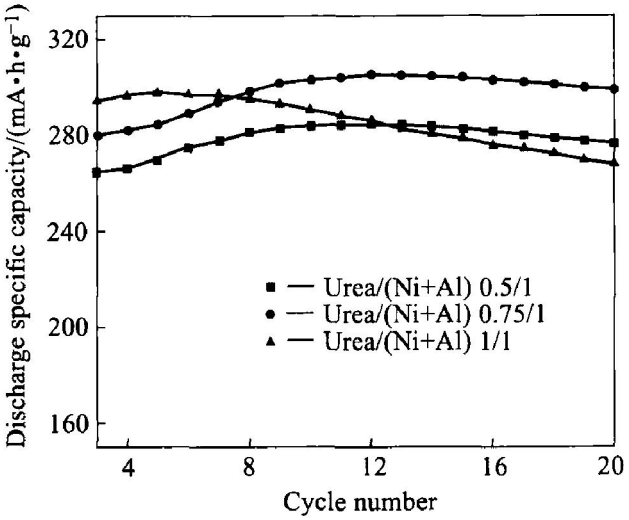

Fig. 10 Specific discharge capacities of Al-substituted α-Ni(OH)$_2$ prepared at different reagent ratios

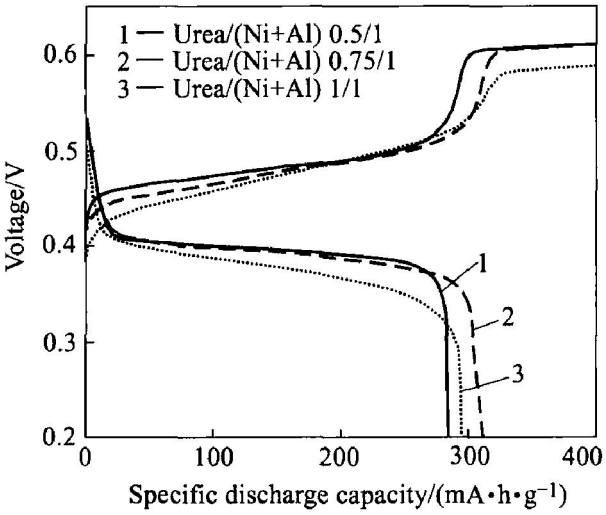

Fig. 11 Charge-discharge curves of Al-substituted α-Ni(OH)$_2$ prepared at different reagent ratios

stability of the samples. The diffraction peaks signed with asterisk and diamond symbol are assigned to binder PTFE and substrate foam nickel, respectively. It can be seen that the diffraction peaks of Al-substituted α-Ni(OH)$_2$ shift to large angle side, which suggests that its interlaminar distance decreases. It is clear that, however, the α-Ni(OH)$_2$ structure is retained after 30 charge-discharge cycling. This shows that Al-substituted α-Ni(OH)$_2$ prepared by homogeneous precipitation method are stable in electrochemical cycling process. Liu et al[6] also found that 25% and 20% Al-substituted αNi(OH)$_2$ prepared by chemical precipitation method were stable.

3.4 Effect of molar ratio of urea to (Ni+ Al) ions

The molar ratio of urea to (Ni+ Al) ions is set at 0.5∶1, 0.75∶1 and 1∶1 and other reaction conditions are 104 ℃ of reaction temperature and 4 h of reaction time. The discharge capacity is shown in Fig. 10. It can be seen that when the ratio of urea to (Ni + Al) ions is 0.75∶1, Al-substituted α-Ni(OH)$_2$ has the largest capacity. With the ratio of urea to (Ni+ Al) ions increasing, the charge and discharge potential decreases slightly. For charge potential, this difference is more notable when the capacity is less than 180 mA·h/g. With the discharging proceeding, the difference between the discharge potential becomes larger. For all samples, the oxygen evolution occurs at the state of charge (SOC) of 100% (Fig. 11), which suggests that charge efficiency of samples is high.

3.5 Impedance experiment

The impedance spectra of α-type nickel hydroxide electrode with a state of charge of 20%–100% are shown in Fig. 12. The characteristics of impedance are similar to β-type electrode. The Nyquist plot is composed of two parts: the semicircle in the high-frequency range followed by a straight line that is almost perpendicular to real axis. The semicircle in the high frequency region has characteristic of the charge-transfer resistance (R_2) acting in parallel with the double-layer capacitance (Q_1). The diameter of the semicircle reflects the magnitude of charge-transfer resistance (R_2). The straight line in intermediate-low frequencies is due to proton diffusion in the solid phase where a higher slope signifies a faster rate of diffusion. In the limited situation, the slope is infinite, i.e. the straight line is perpendicular to real axis which is characterized by finite diffusion in solid phase. In the range of SOC< 80%, the error between fitting

data and experimental results is large with the solid state infinite diffusion model because the straight line is not completely perpendicular to real axis. Therefore the low frequency results are directly described with the slope. As seen from Fig. 12 that with SOC increasing, the slope increases, which suggests a faster rate of diffusion. The semicircle at high frequencies is compressed so that its center is below real axis. Therefore, to fit the data, an equivalent circuit model containing constant phase element(CPE) Q should be used. Its impedance is described as[18, 19]

$$Z_{CPE} = \frac{1}{Y(j\omega)^n} \quad (3)$$

where ω is the angular frequency in rad/s, Y and n are adjustable parameters of CPE. For planar electrode, a value of $n = 1$ corresponds to capacitance, $n = 0$ corresponds to resistance and $n = 0.5$ corresponds to Warburg diffusion. Many researchers reported compressed semicircle and it happened generally in porous electrode. The reason for this is probably nonuniformity of current density. The equivalent circuit of electrode process at high frequency is shown in Fig. 13 and the fitting data are listed in Table 4. According to the results in Table 4, with the state of charge(SOC) increasing, the charge-transfer resistance (R_2) decreases. The charge-transfer resistance (R_2) is influenced by many factors including reaction active energy. The

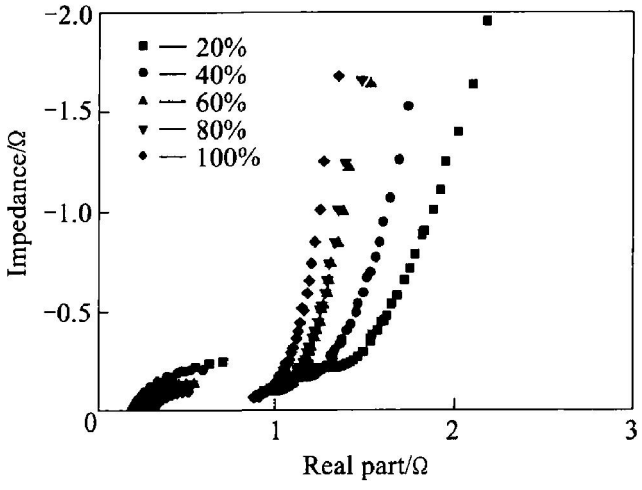

Fig. 12 Impedance of nickel hydroxide electrode (Preparation condition: reagent concentration 0.42 mol/L, reaction temperature 104 ℃, reaction time 4 h, ratio of urea to (Ni+ Al) ions 1∶1)

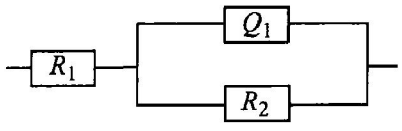

Fig. 13 Equivalent circuits of α-Ni(OH)$_2$ electrode at high frequency for impedance spectra

Table 4 Values of equivalent circuit parameters for data of α-Ni(OH)$_2$ electrode

SOC/%	R_1/Ω	R_2/Ω	Q	n
20	0.23	0.9	0.056	0.62
40	0.19	0.68	0.047	0.69
60	0.25	0.46	0.063	0.67
80	0.26	0.44	0.06	0.69
100	0.30	0.34	0.11	0.64

electrode potential increases and reaction active energy decreases with SOC increasing, therefore charge-transfer reaction proceeds easier.

4 CONCLUSIONS

In this paper, the single-phase Al-substituted α-Ni(OH)$_2$ samples were obtained by homogeneous precipitation method under different preparation conditions. All the samples have higher crystallinity. The samples prepared at 100 and 104 ℃ have larger specific discharge capacity of 320 mA · h/g and lower charge potential than those prepared at 90 and 95 ℃. With the increase of reaction time, the specific discharge capacity increases first and then decreases slightly and reaction time 12 h is the optimum. Lower reagent concentration and molar ratio of urea to (Ni+ Al) ions are in favor of better electrochemical performance of Al-substituted α-Ni(OH)$_2$. And the appropriate values are 0.42 mol/L (Ni+ Al) ions concentration and 0.75∶1 molar ratio, respectively. The sample is stable in the electrochemical cycling process.

REFERENCES

[1] Bode H, Dehmelt K, Witte J. Theory of the nickel hydroxide electrode—I about the nickel(Ⅱ)—hydroxidhydrat [J]. Electrochim Acta, 1966, 11: 1079-1087. (in Germany)

[2] Faure C, Delmas C, Fouassier M. Characterization of a turbostratic α-nickel hydroxide quantitatively obtained from an $NiSO_4$ solution [J]. J Power Sources, 1991, 35: 279-290.

[3] Indira L, Dixit M, Kamath P V. Electrosynthesis of layered double hydroxides of nickel with trivalent cations [J]. J Power Sources, 1994, 52: 93-97.

[4] Delmas C, Faure C, Borthomieu Y. The effect of cobalt on the chemical and electrochemical behaviour of the nickel hydroxide electrode [J]. Mater Sci, 1992, B13(2): 89-96.

[5] ZHANG Qian, XU Yan-hui, WANG Xiao-lin. The structure and electrochemical performance of Al-doped α-Ni(OH)$_2$[J]. Rare Metal Mat Eng, 2003, 32(10): 825-828. (in Chinese)

[6] LIU Bing, ZHANG Yun-shi, YUAN Hua-tang, et al. Electrochemical studies of aluminum substituted α-

$Ni(OH)_2$ electrodes [J]. Int J Hydrogen Energ, 2000, 25: 333－337.

[7] Faure C, Delmas C. Preparation and characterization of cobalt-substituted α-nickel hydroxide stable in KOH medium (Part Ⅱ) —α-hydroxide with a turbostratic structure [J]. J Power Sources, 1991, 35: 263－277.

[8] XU Yan-hui, CHEN Chang-pin, WANG Xiao-lin, et al. The structure and electrochemical properties of ball-milled $Ti_{0.9}Zr_{0.2}Mn_{1.6}Ni_{0.2}V_{0.2}$ alloys [J]. Solid State Ionics, 2002, 146: 57－161.

[9] Yang J, Ciureanu M, Roberge R. Hydrogen storage properties of nano-composites of Mg and Zr-Ni-Cr alloys [J]. Mater Lett, 2000, 43: 234－239.

[10] XU Yan-hui, HE Guo-rong, WANG Xiao-lin. Hydrogen evolution reaction on the AB_5 metal hydride electrode [J]. Int J Hydrogen Energ, 2003, 28: 961－965.

[11] YUAN Xian-xia, XU Nai-xin. Effects of particle size on electrochemical performance of $MlNi_{3.65}Co_{0.75}Mn_{0.4}Al_{0.2}$ [J]. Rare Metal Mat Eng, 2001, 30: 306－309. (in Chinese)

[12] Porta F, Recchia S, Bianchi C, et al. Synthesis and full characterisation of nickel(Ⅱ) —colloidal particles and their transformation into NiO [J]. Colloid Surface A, 1999, 155: 395－404.

[13] Biljana P, Tanja K, Metodija N, et al. A solution growth route to nanocrystalline nickel oxide thin films [J]. Appl Surf Sci, 2000, 165: 271－278.

[14] Akinc M, Jongen N, Lemaître J, et al. Synthesis of nickel hydroxide powders by urea decomposition [J]. J Eur Ceram Soc, 1998, 18: 1559－1564.

[15] XIA Xi, WEI Ying. Preparation and charge/discharge performance of nano-β-$Ni(OH)_2$ [J]. J Inorg Mater, 1998, 13: 674－678. (in Chinese)

[16] ZHANG Qian, XU Yan-hui, WANG Xiao-lin. Preparation of Al-doped α-$Ni(OH)_2$ by homogeneous precipitation and its electrochemical performance [J]. Rare Metal Mat Eng, 2004, 33(12): 1291－1294. (in Chinese)

[17] LIU Guang-hua, PAN Ji-luan. Modern Material Chemistry [M]. Shanghai: Shanghai Science and Technology Press, 2000.

[18] Viswannathan V V, Salkind A J, Kelley J J, et al. Effect of state of charge on impedance spectrum of sealed cells(Ⅰ) —Ni-Cd cells [J]. J Appl Electrochem, 1995, 25(8): 716－728.

[19] Brug G L, van den Eden A L G, Rehbach M S, et al. Analysis of electrode impedances complicated by the presence of a constant phase element [J]. J Electroanal Chem, 1984, 176: 275－295.

(Edited by YANG Bing)